Available online at www.sciencedirect.com
SCIENCE DIRECT®
Pergamon
Cement and Concrete Research 34 (2004) 1451–1457
CEMENT AND CONCRETE RESEARCH

The correlation between compressive strength and ultrasonic parameters of calcium aluminate cement materials

T. Matusinović*, S. Kurajica, J. Šipušić

Faculty of Chemical Engineering and Technology, Department of Inorganic Chemical Technology and Nonmetals, University of Zagreb, Marulićev trg 20, HR-10000 Zagreb, Croatia

Received 23 January 2003; accepted 29 January 2004

Abstract

Calcium aluminate cement (CAC) mortars were investigated by nondestructive ultrasonic measurement in the through-transmission mode and compressive strength measurements. The detected profile of ultrasonic signal was fitted as a sine wave modulated with the Gauss function. The linear relationship between compressive strength and the product of the amplitude and angular frequency of the signal was established. A qualitative explanation of the proposed correlation based on the existing theories was given.

Keywords: Hydration; Compressive strength; Calcium aluminate cement; Lithium compounds; Ultrasound

1. Introduction

There is a continuous need to evaluate the state of the concrete structures already in use (like bridges, tunnels, dams, buildings, etc.) [1]. Nondestructive methods of investigation, such as ultrasonic measurements, are often proposed. The use of ultrasonic methods in cement materials investigations dates more than 40 years ago on both Portland and other special cements [2]. The usual parameter measured is the velocity of longitudinal ultrasonic waves in material that, together with the density, enables calculation of Young's modulus of elasticity. The velocities of transversal and surface ultrasonic waves are also measured and relations between thus obtained ultrasonic parameters and bulk elastic modulus of material can be found [3–5]. The influence of aggregate to cement ratio on the compressive strength–ultrasonic pulse velocity dependence had been shown [3,6]. Popovics et al. [7] presented clear experimental evidence that compressive strength is dependent on concrete composition (that is, different concretes have different calibration curves) and additional results stressed the complex properties of concrete, role of compositeness and dispersion are discussed. The conclusion that evolved over years, about correlations between velocity of ultrasonic waves and compressive strength of cement materials is that some additional properties have to be measured, for example, hammer rebound index, hardness, etc. [3]. Recently, several studies of cement and concrete setting and hardening by ultrasonic measurements have been published [8–10]. In those studies, compressive strength of samples was not investigated. The correlation between compressive strength and ultrasonic pulse velocity, proposed for calcium aluminate cement (CAC) mortars has the form of either power law or exponential function [11,12]. It was pointed out that proposed correlation should be used for similar materials compositions only. Liang and Wu [13] have recently presented theoretical justification for the exponential dependence of strength on velocity. They have also made one step in further developing the combined method that includes both measured ultrasonic pulse velocity and amplitude in predicting the compressive strength of concrete. The preceding literature overview points out that there exist some limitations regarding the possibility of establishing a general relation between compressive strength and velocity of ultrasonic waves for cement materials. The aim of this work was to extract information from the profile of ultrasonic signal, thus monitoring the evolution of properties of CAC materials at early ages and to correlate them with the compressive strength of material.

* Corresponding author. Tel.: +385-1-4597-218; fax: +385-1-4597-250.
E-mail address: tmatusin@pierre.fkit.hr (T. Matusinović).

0008-8846/$ – see front matter © 2004 Elsevier Ltd. All rights reserved.
doi:10.1016/j.cemconres.2004.01.024

2. Theoretical background

Several approaches describing/dealing with the problem of ultrasonic wave propagation through cement materials are described. Recent work of Liang and Wu [13] deals with the wave propagation in cement materials. Depending on the boundary conditions, solution to the one-dimensional ultrasonic wave propagation Eq. (1) gives velocity of longitudinal wave, v_L/ms^{-1}, $v_L=((E/\rho)f(v))^{1/2}$, where E is Young's modulus, ρ is the density of the material and $f(v) \approx 1$ is a function of the Poisson's ratio.

$$\frac{\partial^2 u}{\partial t^2} = \frac{E}{\rho} f(v) \frac{\partial^2 u}{\partial x^2} \tag{1}$$

Eq. (1) is of the form $(\partial^2 u/\partial t^2)=(\text{constant})^2(\partial^2 u/\partial x^2)$ because it is supposed that material could be described as homogenous, and its properties does not depend on time or distance. Choice of different material or boundary condition would change the values of Young's modulus and density (material properties) or $f(v)$, respectively. A more general form of wave Eq. (1) is the so-called telegraph Eq. (2) [13]:

$$\frac{\partial^2 u}{\partial t^2} = \frac{E}{\rho} f(v) \frac{\partial^2 u}{\partial x^2} + p \frac{\partial u}{\partial t} + qu \tag{2}$$

Two new terms are added corresponding to a damping force, $p(\partial u/\partial t)$, whereas the term qu produces wave dispersion. Harmonic wave propagating through the viscous material attenuates (due to the energy dissipation), and its frequency is lower, Eq. (3) [14]:

$$\omega = \sqrt{\omega_0^2 - \delta^2} \tag{3}$$

Micromechanics approach has been applied by Hernández et al. [15] to the characterization of mortars by ultrasound. In their approach, representative volume element of a composite material is formed by an isotropic elastic matrix of volume V^m and ellipsoidal nonhomogenous inclusions of volume V^i. Averaging material properties, two independent tensor's elastic constants C_{11} and C_{44} are calculated by knowing unporous matrix constants C_{11}^m and C_{44}^m and pore volume fraction. The velocity of longitudinal ultrasonic wave, v_L equals Eq. (4):

$$v_L = \sqrt{\frac{C_{11}}{\rho}} \tag{4}$$

and shear wave velocity, v_S equals Eq. (5):

$$v_S = \sqrt{\frac{C_{44}}{\rho}} \tag{5}$$

From calculated values of composite's elastic constants C_{11} and C_{44}, the Young's modulus can also be calculated, Eq. (6):

$$E = \frac{C_{44}(3C_{11} - 4C_{44})}{C_{11} - C_{44}} \tag{6}$$

The compressive strength of a composite material (concrete) is calculated from the empirical dependence of the compressive strength on Young's modulus. Berthaud [5] also mentioned the possibility of deducing the evolution of the Young's modulus and Poisson ratio from the measurements of longitudinal and shear wave velocity. Panet et al. [16] applied micromechanics model in the study of ageing of cement material. They call for improved modeling taking into account wave diffusion on cracks, pores and aggregates.

Velocity of elastic waves enables to learn several aspects of materials [5]:

- elastic constant if the wavelength is large when compared to the size of heterogeneity,
- their internal structure if the wavelength is short when compared to the size of the heterogeneity.

Wave propagation event, through relatively simple two-phase systems (suspensions of particles in gas [17] or liquid [18]), are governed with complex models and resulting solutions.

Recently, Haire and Langton [19] had reviewed Biot theory that is applicable to the wave propagation through the fluid-saturated porous media. Although Biot theory had great success in many of its applications, it has been found in some instances to be only an approximation, possibly in cases when additional attenuation mechanisms are operative (e.g., in the case of complex pore shapes). Incomplete knowledge of the material's properties that are needed for calculations is likely to occur in the case of time-dependent properties of cement materials. Nilsen and Monteiro [20] had shown evidence that concrete and mortar behave as a three-phase material consisting of the cement matrix, sand particles and interfacial transition zone (ITZ), while Yang [21] has shown the influence of the ITZ on the elastic module of mortar. Chaix et al. [1] have analyzed back-scattered ultrasonic waves from the concrete material consisting of numerous scatterers (sand particles) giving rise to the received signal, that is, a superposition of large number of elementary (single) reflection events in spatial/temporal domain. Their model of the structure is very instructive because as for every wave that impinges phase boundary (two materials of different acoustic impedances, $Z=\rho v$), part of the wave's energy is transmitted and reflected. Thus, the transmitted ultrasonic wave is a superposition of large number of waves differing in phase and intensity. The result is a voltage–time curve as obtained using piezoelectric ultrasonic receiver (transducer).

Recent studies [22–24] of the wave propagation in nonlinear elastic materials, such as rocks and sandstones, enable new insights in the interpretation of the results of ultrasonic measurements. It has been shown that volumetrically damaged material, like concrete, possesses nonlinear elastic properties, and one manifestation of nonlinearity is the shift of ultrasound frequency towards lower frequencies. If more cracks and microcracks are present in the material, the frequency shift is greater.

As the strength of concrete also depends on the number and size of (critical) cracks [25–27], the measured compressive strengths should correlate with the extent of nonlinear elastic response as determined by ultrasonic measurements. The frequency shift has contributions from both linear (Eq. (3)) and nonlinear effects.

Because of the aforementioned problem of microscopic description and modeling of ultrasonic wave propagation through porous polyphase composite material, we sought for a way of obtaining easily measurable parameters from the transmitted ultrasonic signal representative for the macroscopic state and properties of the material.

3. Methods

The CAC used was taken from a regular production of "Istra Cement International," Pula, Croatia, part of Heidelberger Zement Group. The cement has the following oxide mass fraction composition: CaO, 40.2%; Al_2O_3, 39.0%; Fe_2O_3, 11.7%; FeO, 4.3% and SiO_2, 1.9%. The principal mineral phase is monocalcium aluminate, $CaAl_2O_4$ (CA), with $Ca_{12}Al_{14}O_{33}$ ($C_{12}A_7$), $Ca_4Al_2Fe_2O_{10}$ (C_4AF) and β-Ca_2SiO_4 (β-C_2S) as minor phases. Li_2CO_3 used was commercial analar grade reagent.

Two different compositions of CAC mortars were prepared at w/c ratio of 0.44 and 20 °C as described in Refs. [28–30]. Sample S31 had a quartz sand (fraction: 0.63–1.25 mm) to cement ratio of 3:1. Sample S21L had a standard sand to cement ratio of 2:1 with Li_2CO_3 added as a setting accelerator. Samples were investigated by ultrasonic measurements in through-transmission mode under immersion (Fig. 1) and by compressive strength determination according to EN 196-1. The ultrasonic probes used were K0.5S/B0.5SL operating at 500 kHz frequency and were driven by spike impulse at a repetition frequency of 100 Hz. Transient signals were measured using LeCroy 9310 AM oscilloscope.

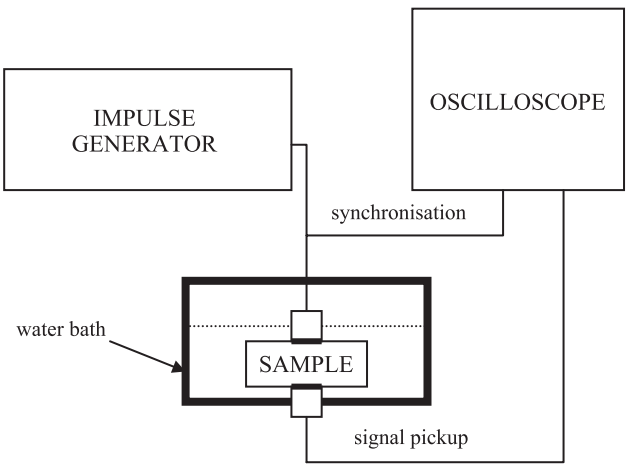

Fig. 1. Ultrasonic measurements setup.

4. Results and discussion

Nondestructive ultrasonic measurements and compressive strength measurements were conducted on samples S31 and S21L during the first 10 h of hydration. Sample S21L started to develop strength approximately 3 h earlier than the sample S31 due to the addition of lithium carbonate accelerator [28]. Compressive strength of the sample S31 is lower than the compressive strength of the sample S21L because of the narrow quartz sand particle size distribution and entrapped air voids within the material. Hydration of CAC proceeds through the dissolution of CA and subsequent precipitation of calcium aluminate hydrates and alumina gel. Products of reaction between CA and water have greater volume than CA alone and they bind together filling the space between grains, which is accompanied by an increase of strength and a decrease of porosity [29,30].

Measured ultrasonic signals for selected times of hydration for the sample S21L are presented in Fig. 2. From Fig. 2, it is seen that as the hydration advances, the amplitude of the ultrasonic signal increases and the time of flight of the wave packet decreases (shift of the voltage–time curves to the left). Decrease of the time of flight of the received longitudinal ultrasonic pulse corresponds with the increase of the longitudinal wave group velocity. Thus, as hydration of the sample advances, the porosity decreases while the increase in compressive strength, ultrasonic pulse amplitude and velocity is observed.

The usual procedures of the ultrasonic signal interpretation extract the time of flight of the ultrasonic wave and the amplitude of the signal. That is, only three points are used from the whole signal that contains typically about thousand $U(t)$/V points. The functional form that fits a measured ultrasonic signal could provide additional information. The aim of this work was to find the additional parameters from the ultrasonic signal received that could be correlated with the compressive strength of the material (CAC mortar samples). Various functions were tested and the best fit of the voltage–time curves was obtained for a sine wave modulated with the Gauss function (Eq. (7)):

$$U(t) = A\sin(\omega t - \varphi)\exp\left(-\frac{(t-t_c)^2}{w^2}\right) \quad (7)$$

where A/V is amplitude of the signal envelope, ω/rad $^{-1}$ is the angular frequency of the wave, φ/rad is the phase shift

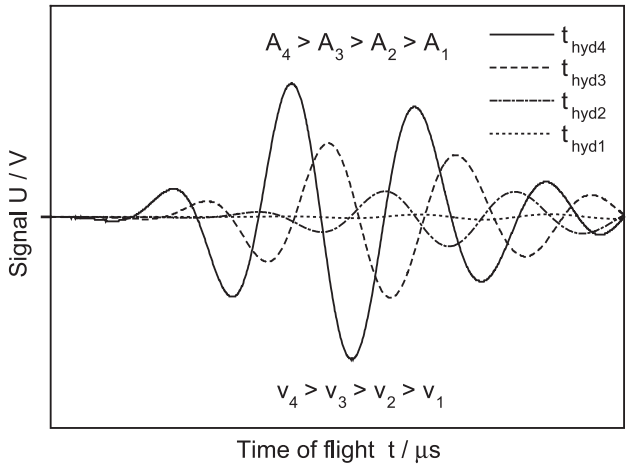

Fig. 2. Increase of amplitude (A) and velocity (v) of ultrasonic waves at prolonged time of hydration, $t_{hyd4}>t_{hyd3}>t_{hyd2}>t_{hyd1}$. Experimental data for S21L at hydration times $t_{hyd1}=133$ min, $t_{hyd2}=141$ min, $t_{hyd3}=158$ min and $t_{hyd4}=172$ min.

of the wave, t_c/s is the time of the arrival of the wave packet group velocity and w/s is the width of the distribution. That functional form could be found in a textbook by Henc-Bartolic [14] and is similar (in a different notation) as the one used by Chaix et al. [1] to describe incident ultrasound wave. Eq. (7) is shown schematically in Fig. 3. From the figure, it is seen that the wave packet is represented as sinusoidal wave of the angular frequency, ω/s^{-1}, modulated with the Gauss function.

The measured ultrasonic signals for the two investigated samples at different times of hydration were fitted to the proposed function and the results are presented in Tables 1 and 2. Good agreement between experimental and fitted data is shown in Figs. 4 and 5 for the sample S31 at 482 min of hydration and sample S21L at 289 min of hydration. Values of the parameters of Eq. (7), along with the error margins and square of S.D., are listed in Table 3. S.D. between fitted and experimental data is less than 0.5% of

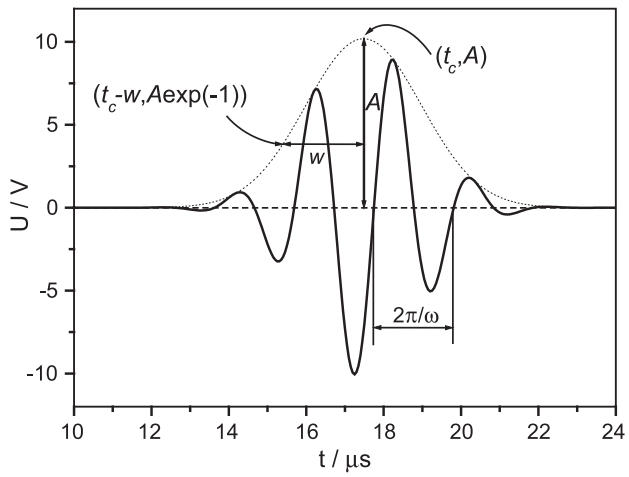

Fig. 3. Function $U(t)=A\sin(\omega t-\varphi)\exp(-(t-t_c)^2/w^2)$ shown schematically. $A=10.17$ V, $\omega=3.02\times10^6$ s^{-1}, $\varphi=0.81$ rad, $t_c=17.41$ µs, $w=2.08$ µs.

Table 1
Results of fit of Eq. (7) on the measured $U(t)$ ultrasonic signal at different times of hydration, t_{hyd}/min, for the sample S31

t_{hyd}/min	A/V	t_c/µs	w/µs	$\omega\ 10^{-6}$/rad^{-1}	φ/rad
265	0.044	23.24	3.43	2.06	4.51
269	0.069	23.03	3.32	2.09	4.26
271	0.091	22.95	3.25	2.12	4.10
275	0.182	22.23	3.06	2.23	3.40
278	0.231	22.09	3.01	2.26	3.26
280	0.285	21.96	2.97	2.28	3.15
289	0.631	21.61	2.77	2.41	2.05
300	1.171	20.57	2.61	2.51	2.46
308	1.555	20.21	2.54	2.57	2.25
318	1.825	19.73	2.42	2.64	2.14
335	2.486	19.13	2.28	2.72	2.05
365	4.968	17.98	2.23	2.83	2.94
378	5.267	17.71	2.23	2.84	2.95
392	6.657	17.40	2.19	2.88	3.37
407	6.973	17.17	2.20	2.90	3.63
426	8.100	16.94	2.19	2.93	3.80
441	8.280	16.83	2.18	2.95	3.86
455	9.330	16.64	2.17	2.98	3.90
482	10.21	16.29	2.16	3.00	4.20
515	11.33	16.26	2.18	3.03	4.10
536	11.60	16.13	2.16	3.03	4.26
548	11.63	16.08	2.18	3.05	4.14
559	11.81	16.03	2.18	3.06	4.19
572	11.55	16.08	2.22	3.08	3.93

Table 2
Results of fit of Eq. (7) on the measured $U(t)$ ultrasonic signal at different times of hydration, t_{hyd}/min, for the sample S21L

t_{hyd}/min	A/V	t_c/µs	w/µs	$\omega\ 10^{-6}$/rad^{-1}	φ/rad
133	0.040	23.60	2.65	2.62	−0.87
139	0.267	22.91	2.52	2.72	−0.88
141	0.425	22.48	2.49	2.67	−0.08
158	1.183	20.92	2.34	2.74	−1.55
160	1.358	20.77	2.34	2.74	−1.41
172	2.104	19.93	2.22	2.82	−0.97
174	2.361	19.79	2.20	2.83	−0.90
184	3.725	19.21	2.23	2.87	−0.31
187	3.967	19.13	2.24	2.88	−0.23
194	4.725	18.84	2.28	2.90	0.13
204	5.691	18.28	2.09	2.94	0.20
213	6.800	18.24	2.19	2.98	0.35
222	7.862	17.73	2.18	3.00	0.94
229	8.645	17.64	2.17	3.00	1.15
238	10.18	17.48	2.11	3.05	0.81
250	11.15	17.46	2.15	3.07	0.97
272	13.45	16.87	2.08	3.12	1.31
280	14.67	16.66	2.03	3.11	1.55
289	15.90	16.48	2.02	3.13	1.56
301	15.98	16.33	2.02	3.14	1.75
320	17.77	16.25	2.04	3.17	1.52
352	19.12	16.12	2.07	3.19	1.61
363	19.32	16.06	2.07	3.20	1.62
375	19.98	16.00	2.09	3.18	1.88
394	20.41	15.99	2.08	3.19	1.80
404	20.22	15.94	2.08	3.18	1.94
411	21.00	15.93	2.09	3.19	1.94
427	21.07	15.75	2.00	3.20	1.96

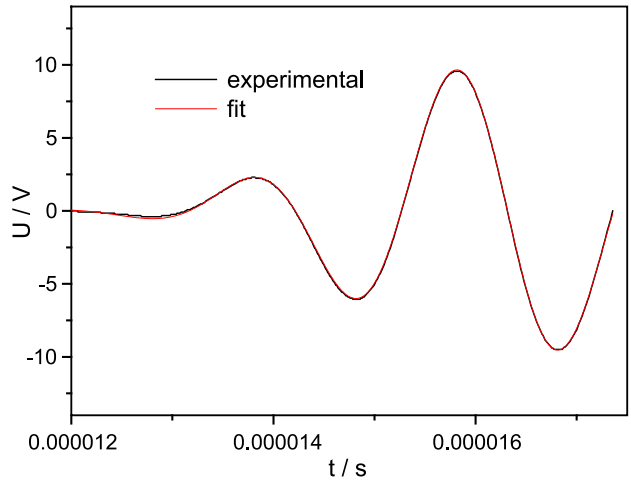

Fig. 4. Experimental and fitted data for the sample S31 hydrated 482 min.

signal span for all the measured datasets. From Tables 1 and 2, it is seen that the amplitude of the signal increases as the hydration advances. The increase of the amplitude of the ultrasonic signal is a consequence of the decrease of the porosity that acts as a scatterer and the decrease of the quantity of the liquid phase that is a source of viscous damping. From Tables 1 and 2, it can be also seen that the angular frequency of the signal increases and the angular frequency shift (the difference between the angular frequency of the ultrasonic probe and angular frequency of the signal) decreases. The difference between ultrasonic probe's nominal frequency (54 kHz) and peak frequency of the Fourier Transformed received signal (47 kHz) was noticed by Popovics et al. [7], but was not commented further. The decrease of the frequency shift could be explained as a consequence of the linear and nonlinear elastic response of the material under study. In the realm of linear elastic behavior, frequency shift occurs because of the viscous damping. The decrease of viscous damping during hydration decreases frequency shift (Eq. (3)). From the nonlinear elastic behavior view [22–24], decrease of the angular

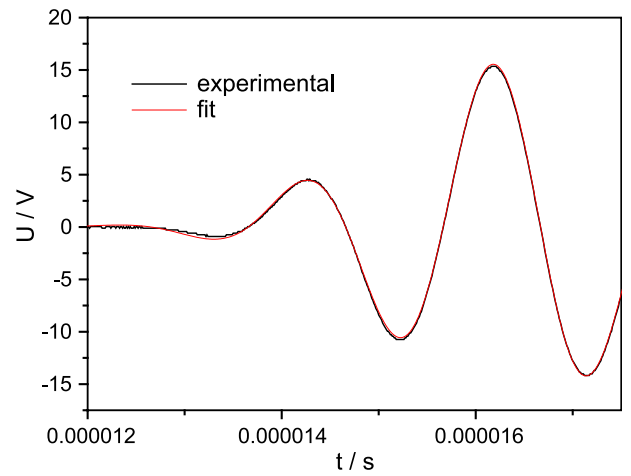

Fig. 5. Experimental and fitted data for the sample S21L hydrated 289 min.

Table 3
Values of the parameters of Eq. (7) for the best fit obtained for the sample S31 at 482 min of hydration and S21L for 289 min of hydration

	S31	S21L
A	10.216 ± 0.011	15.908 ± 0.024
ω	2.9923 ± 0.0007	3.1274 ± 0.0010
φ	4.205 ± 0.008	1.561 ± 0.012
t_c	16.288 ± 0.002	16.479 ± 0.003
w	2.157 ± 0.003	2.023 ± 0.004
S.D.[2]	0.00388	0.01857

frequency shift during hydration is a consequence of more dense structure that develops, with less defects and microcracks.

The product of amplitude and angular frequency ($A\omega$/Vs^{-1}) is in fact proportional to the maximum velocity of particles of the material [14]. Ultrasonic wave propagation through the cement material at later ages of hydration induces greater velocities of the particles of the material and the rate of the change of momentum is greater. Thus, cement material at later ages of hydration have greater ability to carry stress, or alternatively, greater ability to transfer force. Results of compressive strength measured plotted against the product of amplitude and angular frequency ($A\omega$/Vs^{-1}) is shown in Fig. 6. As could be seen, the linear dependence for the samples investigated is obtained. The products of A and ω are interpolated from the measured data (Tables 1 and 2) at the time of hydration, t_{hyd}, that corresponds to the compressive strength determination and are presented in Table 4. The data of compressive strengths measured against the product $A(t_{hyd})\omega(t_{hyd})$ were fitted as a straight line (S.D. of 2 MPa) through the origin because the compressive strength and the $A\omega$ product of fresh CAC mortar are practically 0. The different slopes of the lines are caused by the different coefficients of absorption of ultrasound in mortars, because of different sand to cement ratios and probably different surface roughnesses that influence

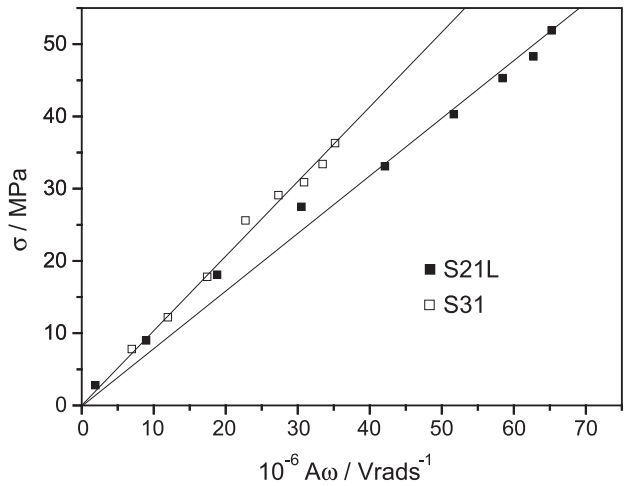

Fig. 6. Results of compressive strength measured plotted against the product of amplitude and angular frequency ($A\omega$/Vs^{-1}) show linear dependence for the samples investigated.

Table 4
Compressive strengths of the samples S31 and S21L measured and the product of amplitude and circular frequency ($A\omega$/V rad^{-1}) interpolated at times of hydration, t_{hyd}/min

S31			S21L		
t_{hyd}/min	$A\omega 10^{-6}$/ V rad^{-1}	σ/MPa	t_{hyd}/ min	$A\omega 10^{-6}$/ V rad^{-1}	σ/MPa
330	6.96	7.8	150	1.89	2.8
360	11.96	12.2	180	8.95	9.0
390	17.43	17.8	210	18.79	18.1
420	22.73	25.6	240	30.51	27.5
450	27.32	29.1	270	42.10	33.1
480	30.88	30.9	300	51.66	40.3
510	33.44	33.4	330	58.42	45.3
540	35.17	36.3	360	62.71	48.3
			390	65.23	51.9

sample/probe contact. The samples of constant thickness were used but it is worth noting that different thicknesses of the same material would result in different amplitudes (because of the attenuation) and therefore different slopes of the line of linear fit.

Although CAC mortars investigated differ greatly in aggregate to cement ratio, aggregate particle size distribution, setting time due to the addition of Li_2CO_3, the compressive strengths measured were successfully correlated with the ultrasonic parameters of materials. In this way, instead of the usual dependence of compressive strength on the velocity of ultrasonic waves, the compressive strength was correlated with the velocity of particles of the material. Moreover, the information was extracted from the full signal collected.

We suppose that further development will result in three possible applications: monitoring of material condition, especially of concrete materials subjected to the chemically harsh and corrosive environment, qualitative and quantitative assessment of the construction that suffered fire, freeze/thaw or earthquake damage or is simply under heavy exploitation conditions. Possible uses could be found in application to the preservation of archeologically and historically important buildings/cultural heritage. By simply measuring material response (fast and nondestructive ultrasonic measurements), one can compare material homogeneity/uniformity or monitor deterioration of material properties during time. Furthermore, we believe that it will trigger more investigations on the relation between concrete attenuation coefficient and structure thus leading to the better understanding of the concrete as a polyphase composite material.

5. Conclusion

Calcium aluminate mortars prepared were investigated by nondestructive ultrasonic measurement in through-transmission mode and compressive strength determination. By using Eq. (7) for the ultrasonic signal fit, meaningful parameters could be obtained, e.g., ultrasonic pulse group velocity and angular frequency. Frequency shift could be explained as a contribution from linear and/or nonlinear elastic response. Experimental results demonstrated that frequency shift decreases with the advance of hydration, indicating the change of microstructure and development of more dense structure with less defects and microcracks. Linear proportionality of the compressive strength and the maximum velocity of particles of material corresponding to the longitudinal ultrasonic pulse had been proposed (Eq. (8)).

$$\sigma \propto A\omega \tag{8}$$

Particle velocity depends on the frequency shift and on the coefficient of absorption of ultrasound that both depend on the mechanism of wave–microstructure interaction. We suggest that this finding may also be true for other cement materials and other similar materials.

Acknowledgements

The authors acknowledge financial support from the Croatian Ministry of Science and Technology.

References

[1] J.F. Chaix, V. Garnier, G. Corneloup, Concrete damage evolution analysis by backscattered ultrasonic waves, NDT E Int. 36 (2003) 461–469.
[2] T.D. Robson, High-Alumina Cements and Concretes, Wiley, New York, 1962.
[3] J. Krautkrämer, H. Krautkrämer, Ultrasonic Testing of Materials, Springer Verlag, Berlin, 1990.
[4] L.G. Hwa, G.W. Lee, The influence of water on the physical properties of calcium aluminate oxide glasses, Mater. Chem. Phys. 58 (2) (1999) 191–194.
[5] Y. Berthaud, Damage measurements in concrete via an ultrasonic technique: Part I. Experiment, Cem. Concr. Res. 21 (1991) 73–82.
[6] A.M. Neville, J.J. Brooks, Concrete Technology, Longman Scientific and Technical, Harlow, 1987.
[7] S. Popovics, J.L. Rose, J.S. Popovics, The behaviour of ultrasonic pulses in concrete, Cem. Concr. Res. 20 (1990) 259–270.
[8] M.I. Valič, Hydration of cementitious materials by pulse echo USWR-method, apparatus and application examples, Cem. Concr. Res. 30 (10) (2000) 1633–1640.
[9] T. Chotard, N. Gimet-Breart, A. Smith, D. Fargeot, J.P. Bonnet, C. Gault, Application of ultrasonic testing to describe the hydration of calcium aluminate cement at the early age, Cem. Concr. Res. 31 (3) (2001) 405–412.
[10] A. Smith, T. Chotard, N. Gimet-Breart, D. Fargeot, Correlation between hydration mechanism and ultrasonic measurements in an aluminous cement: effect of setting time and temperature on the early hydration, J. Eur. Ceram. Soc. 22 (12) (2002) 1947–1958.
[11] S.M. Gill, P.F.G. Banfill, E. El-Jazairi, The influence of superplasticising admixtures on ciment Fondu mortars, in: R.J. Mangabhai (Ed.), Calcium Aluminate Cements, E & FN Spon, London, 1990, pp. 113–126.
[12] S.M. Gill, P.F.G. Banfill, E. El-Jazairi, The effect of superplasticisers on the hydration of aluminous cement, 8th International Congress on the Chemistry of Cement, Abla Grafica e Editora Ltda, vol. 4, 1986, 322–327, Rio de Janeiro.

[13] M.T. Liang, J. Wu, Theoretical elucidation on the empirical formulae for the ultrasonic testing method for concrete structures, Cem. Concr. Res. 32 (2002) 1763–1769.
[14] V. Henc-Bartolic, Waves and Optics (in Croatian), Školska knjiga, Zagreb, 1991.
[15] M.G. Hernández, J.J. Anaya, M.A.G. Izquierdo, L.G. Ullate, Application of micro mechanics to the characterization of mortar by ultrasound, Ultrasonics 40 (2002) 217–221.
[16] M. Panet, C. Cheng, M. Deschamps, O. Poncelet, B. Audoin, Microconcrete ageing ultrasonic identification, Cem. Concr. Res. 32 (2002) 1831–1838.
[17] W. Gregor, H. Rumpf, The attenuation of sound in gas–solid suspensions, Powder Technol. 15 (1976) 43–51.
[18] J.S. Tebbutt, R.E. Challis, Ultrasonic wave propagation in colloidal suspensions and emulsions: a comparison of four models, Ultrasonics 34 (1996) 363–368.
[19] T.J. Haire, C.M. Langton, Biot theory: a review of its application to ultrasound propagation through cancellous bone, Bone 24 (1999) 291–295.
[20] A.U. Nilsen, P.J.M. Monteiro, Concrete: a three phase material, Cem. Concr. Res. 23 (1993) 147–151.
[21] C.C. Yang, Effect of the transition zone in the elastic moduli of mortar, Cem. Concr. Res. 28 (1998) 727–736.
[22] K.E.-A. Van Den Abeele, P.A. Johnson, A. Sutin, Nonlinear Elastic Wave Spectroscopy (NEWS) techniques to discern material damage: Part I. Nonlinear Wave Modulation Spectroscopy (NWMS), Res. Nondestruct. Eval. 12 (2000) 17–30.
[23] K.E.-A. Van Den Abeele, J. Carmeliet, J.A. Ten Cate, P.A. Johnson, Nonlinear Elastic Wave Spectroscopy (NEWS) techniques to discern material damage: Part II. Nonlinear Resonance Acoustic Spectroscopy, Res. Nondestruct. Eval. 12 (2000) 31–42.
[24] R.A. Gouyer, P.A. Johnson, Nonlinear mesoscopic elasticity: evidence for a new class of materials, Phys. Today 52 (4) (1999) 30–36.
[25] D.M. Roy, G.R. Gouda, Porosity–strength relation in cementitious materials with very high strengths, J. Am. Ceram. Soc. 56 (10) (1973) 549–550.
[26] J.D. Birchall, A.J. Howard, K. Kendall, Flexural strength and porosity of cements, Nature (289) (1981) 388–390.
[27] N. McN. Alford, A theoretical argument for the existence of high strength cement pastes, Cem. Concr. Res. 11 (4) (1981) 605–610.
[28] T. Matusinović, N. Vrbos, Alkali metal salts as set accelerators for high-alumina cement, Cem. Concr. Res. 23 (1) (1993) 177–186.
[29] T. Matusinović, D. Čurlin, Lithium salts as set accelerators for high-alumina cement, Cem. Concr. Res. 23 (4) (1993) 885–895.
[30] T. Matusinović, N. Vrbos, D. Čurlin, Lithium salts in rapid setting high-alumina cement materials, Ind. Eng. Chem. Res. 33 (11) (1994) 2795–2800.